Molecular & Cellular Proteomics. 2016; 15(1): 246-255

Analysis of mitochondrial proteins in the surviving myocardium after ischemia identifies mitochondrial pyruvate carrier expression as possible mediator of tissue viability

Mariana Fernández-Caggiano‡, Oleksandra Prysyazhna‡, Javier Barallobre-Barreiro§, Ramón CalviñoSantos¶, Guillermo Aldama López¶, Maria Generosa Crespo-Leiro‖, Philip Eaton‡ and Nieves Doménech**,‡‡

‡ Cardiovascular Division, King's College London, The Rayne Institute, and St. Thomas' Hospital, London SE1 7EH, United Kingdom;
§Cardiovascular Division, King's College London James Black Centre, London SE5 9NU, United Kingdom;
¶the Interventional Cardiology Unit,
‖Advanced Heart Failure and Heart Transplant Unit,
***Cardiac Biomarkers Group, Instituto de Investigación Biomédica de A Coruña, Complexo Hospitalario Universitario de A Coruña, As Xubias 84, 15006 A Coruña, Spain*

Abstract
The endogenous mechanisms contributing to tissue survival following myocardial infarction are not fully understood. We investigated the alterations in the mitochondrial proteome after ischemia-reperfusion (I/R) and its possible implications on cell survival. Mitochondrial proteomic analysis of cardiac tissue from an *in vivo* porcine I/R model found that surviving tissue in the peri-infarct border zone showed increased expression of several proteins. Notably, these included subunits of the mitochondrial pyruvate carrier (MPC), namely MPC1 and MPC2. Western blot, immunohistochemistry, and mRNA analysis corroborated the elevated expression of MPC in the surviving tissue. Furthermore, MPC1 and MPC2 protein levels were found to be markedly elevated in the myocardium of ischemic cardiomyopathy patients. These findings led to the hypothesis that increased MPC expression is cardioprotective due to enhancement of mitochondrial pyruvate uptake in the energy-starved heart following I/R. To test this, isolated mouse hearts perfused with a modified Krebs buffer (containing glucose, pyruvate, and octanoate as metabolic substrates) were subjected to I/R with or without the MPC transport inhibitor UK5099. UK5099 increased myocardial infarction and attenuated post-ischemic recovery of left ventricular end-diastolic pressure. However, aerobically perfused control hearts that were exposed to UK5099 did not modulate contractile function, although pyruvate uptake was blocked as evidenced by increased cytosolic lactate and pyruvate levels. Our findings indicate that increased expression of MPC leads to enhanced uptake and utilization of pyruvate during I/R. We propose this as a putative endogenous mechanism that promotes myocardial survival to limit infarct size.

Ischemic heart disease resulting from the obstruction of coronary arteries commonly culminates in myocardial infarction. Although restoring blood flow is necessary to re-establish oxygen and nutrients to the ischemic myocardium, reperfusion itself may promote damage due to exacerbated oxidative stress and inflammation (1). Even when patients survive, the damage caused to the heart typically triggers events leading to heart failure. Unfortunately, there are still no effective interventions for limiting injury after ischemia despite the potential of such therapeutic options to reduce morbidity and mortality.

Laboratory and clinical studies suggest that the post-infarction failing heart is characterized by a diminished capacity to convert chemical energy into mechanical work due to mitochondrial imbalances (2). The primary function of mitochondria is to generate ATP via oxidative phosphorylation, which is used by the heart to meet its significant energy demands. In the well perfused healthy heart, ~70–90% of ATP is via β-oxidation of fatty acids, with most of the remaining amount coming from the oxidation of glucose and lactate (3, 4). However, when oxygen is restricted as occurs during ischemia or sub-optimal reperfusion, there is a metabolic shift with glycolysis becoming the primary mechanism of ATP synthesis (5, 6). This metabolic adaptation is likely to be beneficial because glucose oxidation is more efficient than fatty acid oxidation in terms of oxygen consumption. A complete shift to glucose metabolism reduces oxygen demand by 11–13% (7).

A better understanding of the alterations to the mitochondrial proteome that occur following I/R[1] may provide important clues about how to limit injury. Previous studies demonstrated that the myocardial mitochondrial proteome was altered after I/R (8–10), including changes in the expression of electron transport chain (ETC) and energy-producing proteins (11). However, these studies were carried out with small animals and did not address whether changes in protein expression were modulated by proximity to the infarct and probably analyzed the heterogeneous combination of surviving and dying and the necrotic tissue that complicates the interpretation of any alterations to the proteome.

Here we utilized a large established animal, a porcine model of I/R (12), and focused specifically on changes to the mitochondrial proteome in the peri-infarct border zone that had survived and remained viable. The rationale was that defining changes to the mitochondrial proteome specifically in the surviving myocardium that had been at risk of necrosis may provide new insight to endogenous adaptive mechanisms that limit tissue injury and infarction. Indeed, this strategy allowed us to identify increased expression of several proteins in the surviving peri-infarct border zone. These included BRP44 and BRP44L, which were recently independently identified as subunits 1 and 2 of the mitochondrial pyruvate carrier (MPC) (13, 14). Enhanced mitochondrial pyruvate uptake capability would potentially provide a mechanism of protection against necrosis (15, 16). Consistent with this, we found pharmacological inhibition of the MPC-dependent pyruvate uptake with UK5099 significantly enhanced infarction and worsened recovery of ventricular function in a murine model of I/R. We conclude that strategies to enhance mitochondrial pyruvate uptake in the post-ischemic heart may have therapeutic value and enhance tissue viability.

EXPERIMENTAL PROCEDURES

Porcine Model of I/R Injury

Seventeen 3-month-old pigs were randomly assigned into one of three groups, which included healthy controls (n = 6), ischemia followed by 3 days of reperfusion (3/R, n = 5), or ischemia followed by 15 days of reperfusion (15 I/R, n = 6).

Ischemia was induced by inserting an inflatable catheter and occluding the left anterior descending coronary artery for 120 min. This involved sedation using an intramuscular injection of ketamine (15 mg/kg) and azaperone (2 mg/kg), after which a 6 French sheath was inserted (via the femoral artery and using a Judkins Right 6 French guiding catheter) to the ascending aorta, so to selectively engage the left coronary artery. Then a 0.014-inch intracoronary guide wire was advanced up to the distal left anterior descending coronary artery, and a balloon catheter was inflated in the medial left anterior descending coronary artery for 120 min. All procedures followed the European Agreement of Vertebrate Animal Protection for Experimental Use (86/609).

Hearts were dissected, and a 15-mm transverse slice of 2 cm was taken from above the apex. From this section, an LV tissue was excised 1 cm from the focal ischemic lesion of the left ventricle. The cross-section of tissue taken was collected for an area 1-cm away from the left ventricle-infarcted area and contained endocardium, myocardium, and epicardium. It was collected from here on the basis that it was likely to have avoided necrosis; indeed, subsequent histological analyses of this tissue confirmed its viability. Tissue samples were snap-frozen in liquid nitrogen and stored at −80 °C or conserved in paraffin until processing. Morphological characteristics for pigs included in the experiment are provided in supplemental Table 1. Echocardiographs were performed at baseline, 30 min after the induction of ischemia and before sacrifice to evaluate LV dimensions and function using a MyLab 30Gold ultrasound system (Esaote) and MyLab Desk software (Esaote).

Proteomic Analysis

The mitochondria isolation was performed from 100 mg of left ventricle tissue collected as outlined above. Mitochondria were extracted using a commercial kit (Mitochondria Isolation Kit for Tissue from Thermo Fisher Scientific, Waltham, MA) with minor modifications. 30 μg of protein per sample were loaded and separated on BisTris discontinuous 4–12% polyacrylamide gradient gels (NuPAGE, Invitrogen, Carlsbad, CA). After electrophoresis, gels were silver-stained and excised in seven identical parallel bands across lanes leaving no empty gel pieces behind. All gel bands were subjected to in-gel digestion with molecular grade trypsin (Thermo Scientific) using standard protocols (17).

Mass spectrometry was performed on a nanoACQUITY HPLC (Waters) coupled to an Orbitrap Velos mass spectrometer (Thermo Scientific). Digested peptides were suspended in 200 μl of solution of 1% formic acid and injected on a C18 reverse phase column (10 cm length, 75 μm inner diameter, 1.7-μm particle size, column Acquity BEH nano, Waters). The peptides were eluted and separated from the column with the following gradient: 1–4% of 0.1% formic acid in acetonitrile for 5 min, followed by a gradient of 4–35% of 0.1% formic acid in acetonitrile for 120 min, 35–45% of 0.1% formic acid in acetonitrile for 25 min, and 45–80% of 0.1% formic acid in acetonitrile in 3 min. The flow rate was 250 nl/min. The elution of the peptides from the column was coupled to a nanospray ionization source PicoView (PicoTip^{TM}, New Objective). Vaporizer applied voltage was around 2000 V. Peptide analysis utilized an ion trap LTQ Orbitrap-type Velos mass spectrometer (Thermo Fisher Scientific) with 60,000 *m*/*z* resolution of 400. From each scan the 20 most abundant peptides (minimum intensity of 500 counts) were selected and fragmented using 38% normalized collision energy in the linear ion trap with helium as the collision gas. Primary data were collected with Thermo Xcalibur (version 2.1.0.1140) and analyzed with Thermo Proteome Discoverer (version 1.2.0.208).

MS/MS peak lists were generated by extract_msn.exe and matched to a combined pig and human database (UniProtKB/Swiss-Prot release 2015_02, February 4, 2015, 93,943 protein entries) using Mascot (version 2.3.01, Matrix Science) with Thermo Proteome Discoverer (version 1.2.0.208) as an interface. Carboxyamidomethylation of cysteine was chosen as a fixed modification, and oxidation of methionine was chosen as a variable modification. The mass tolerance was set at 10 ppm for the precursor ions and 1.0 atomic mass units for fragment ions. Two missed cleavages were allowed. Scaffold (version 2.3.01, Proteome Software Inc., Portland, OR) was used to calculate the spectral counts and to validate MS/MS-based peptide and protein identifications. Protein identifications were accepted if they could be established at greater than 99.0% probability with at least two independent peptides. All the proteins identified as mitochondrial in this study are identified as such in the Uniprot database and included in the Mito Carta database.

Human Cardiac Tissue

Cardiac tissue samples were obtained 2 cm away from the scar in explanted hearts of patients with ischemic cardiomyopathy undergoing cardiac transplantation at the A Coruña Hospital. The study was approved by the Galician Ethics Committee for Research. Control tissues were obtained from unused donor hearts from the A Coruña Hospital following guidelines of Spanish Royal Decrees 2070/1999 and 1301/2006, which regulate the acquisition and use of human tissues for clinical and research purposes. Written informed consent was obtained from all patients.

Histochemistry

Paraffin histological sections were stained with hematoxylin and eosin and Masson's trichrome following established protocols. Images were taken on a DP71 Olympus microscope (UPlanFl objective, ×10/0.30 numerical aperture) equipped with a DP71 camera (Olympus, Tokyo, Japan).

Immunohistochemistry

Immunohistochemistry was performed following standard protocols. Goat antibodies against BRP44L (Lifespan Biosciences, Seattle, WA, LS-C-119789) and BRP44 (Abcam, Cambridge, MA, ab116316) were used on tissue paraffin sections (4 μm). The peroxidase/diaminobenzidine ChemMate™ DAKO EnVision™ detection kit (Dako, Glostrup, Denmark) was used to determine antigen-antibody interaction. Images were obtained at room temperature on a BX61 Olympus (UPlanFl objective, ×40/0.95 numerical aperture) equipped with a DP71 camera (Olympus).

Western Immunoblotting Analysis

Immunoblotting was performed according to standard protocols. Briefly, 35 μg of mitochondrial extracts were loaded per lane, separated on 4–12% gradient gel (NuPAGE, Invitrogen), and transferred to nitrocellulose. The quality of the mitochondrial extraction was analyzed with the following antibodies: ATP5A (Abcam, ab110273); TRAP1 (Santa Cruz Biotechnology Biotechnology, Dallas, TX, sc-11436); myogenin (Abcam, ab1835), and myoglobin (GAPDH (Abcam, ab9485)). The proteomic results validation was performed with the following antibodies: BRP44L (Lifespan Biosciences, LS-C-119789); BRP44 (Abcam, ab116316); LONP1 (Abcam, ab103809); HSP60 (Abcam, ab13532), and VDAC1 (Cell Signaling, 4866). Horseradish peroxidase (HRP)-conjugated rabbit anti-mouse (Santa Cruz Biotechnology Biotechnology, sc-358923) and HRP-labeled goat anti-rabbit (Santa Cruz Biotechnology Biotechnology, sc-2030) antibodies were use against the corresponding primary antibody.

Real Time PCR for Cardiac Tissue Samples

A 50-mg sample of cardiac tissue, which was preserved in OCT compound, was collected using a punch, and RNA was extracted using TRIzol reagent (Invitrogen). The RNA was treated with DNase I (Invitrogen) for 30 min at room temperature. Using 2-μg aliquots of RNA, cDNAs were synthesized using the First Strand cDNA synthesis kit (Roche Applied Science, Penzbergh, Germany) with oligo(dT) primers. DNA primers were designed using Primer3′ software, and sequences were as follows: Brp44l (5′-gcatgacagtggaaaacgaa-3′ and 5′-cttttaaggccgcagagttg-3′); Lonp1 (5′-gggtggcatcaaagagaaga-3′ and 5′-ctcagggaaggcgatatcaa-3′); Hsp60 (5′-gatgatgccatgctcttgaa-3′ and 5′-ccttcagcacagctacacca-3′); Vdac1 (5′-gacagcaggaaacagcaaca-3′ and 5′-cggacagcgtcagtttgata-3′), and GAPDH (5′-gacagcaggaaacagcaaca-3′ and 5′-cggacagcgtcagtttgata-3′). All primers were loaded at 600 nm, and 1 μl of cDNA was amplified by duplicate in 10 μl of 1× SYBR Green Mix (Roche Applied Science), using a LightCycler 480 real time thermocycler (Roche Applied Science). The following PCR conditions were set as follows: a denaturing step of 7 min at 94 °C, followed by 45 amplification cycles of 94 °C for 10 s, 60 °C for 10 s, and 72 °C for 10 s. PCR products were tested for melting temperature with a temperature ramp of 2.2 °C/s from 65 to 95 °C and shown to correspond to the expected cloned fragments. GAPDH was used as the reference gene, and relative expression was estimated by the $\Delta\Delta Ct$ method as the average value of each sample normalized against the average value of control pigs.

Statistical and Bioinformatics Analysis

The comparison of the mitochondrial proteome was performed between control samples and 3 I/R or 15 I/R groups. A Dunnett's test was used to indicate significant differences in the peptide count and in the gene expression between groups. Dunnett's test was also performed to determine differences between the values obtained after densitometry analysis. To study the correlation between samples, principal component analysis was carried out. Student's *t* tests were used to compare the ejection fraction before and after the ischemia in the I/R porcine model and the left ventricular developed pressure, LVEP, and

coronary flow in the mouse I/R model. All the statistical analysis was performed using the SPSS software (IBM, Armonk, NY).

MeV-TM4 (version 4.6 Dana-Farber Cancer Institute, Boston, MA) software was used to generate heat maps based on the ontology of the biological processes. Protein spectral counts were standardized across all the samples. Thus, if a specific protein has a spectral count value under the average, it will generate a negative value that will show as a down-regulated protein in the heat map. To assign the gene ontologies, UniProt IDs were transformed to EntrezGene ID using the CNIO ID converter. The EntrezGene IDs were introduced as inputs into the Term AmiGO Enrichment software to find significantly altered biological processes in each experimental condition.

Isolated Mouse Heart Studies Assessing the Impact of MPC Inhibition on I/R Injury

Experiments were performed in accordance with the Home Office "Guidance on the Operation of Animals (Scientific Procedures) Act 1986" published by HMSO (London, UK). Male C57bl6 (Charles River, UK) mice were terminally anesthetized with pentobarbitone (Pentoject, Animalcare, York, UK; 180 mg/kg intraperitoneally with 150 IU heparin, i.p.). Hearts were rapidly excised, placed in ice-cold modified Krebs-Henseleit (K-H) buffer containing (in mmol/liter) NaCl 118.5, $NaHCO_3$ 25.0, KCl 4.7, KH_2PO_4 1.2, $MgSO_4$ 1.27, d-glucose 5.5, sodium pyruvate 2, sodium octanoate 1.2, and $CaCl_2$ 1.4. The aorta was cannulated and retrogradely perfused at a constant pressure of 80 mm Hg with K-H buffer equilibrated with 95% O_2 and 5% CO_2. A fluid-filled balloon inserted into the left ventricle monitored contractile function. The balloon was gradually inflated until the end-diastolic pressure was between 2 and 10 mm Hg. Hearts were then paced at 550 beats/min. After retrograde perfusion commenced, the hearts were stabilized for 40 min. For inclusion, all hearts had to fulfill the following criteria: coronary flow between 2.0 and 3.5 ml/min and left ventricular developed pressure >60 mm Hg. All hearts then underwent 30 min of global ischemia by clamping the aortic inflow tubing, followed by 2 h of reperfusion. Electrical pacing was stopped after 2 min of ischemia (when contraction ceased) and restarted with reperfusion. To assess the contribution of the mitochondrial pyruvate carriers, one cohort was perfused with K-H buffer containing mitochondrial pyruvate carrier inhibitor UK-5099 (50 μm).

At the end of the protocol, hearts were perfused during 3 min with 10 ml of 3% triphenyltetrazolium chloride (Sigma, Dorset, UK) and then placed in an identical solution at 37 °C for 10 min. The atria were then removed, and the hearts were blotted dry, weighed, and stored at −80 °C until analysis (no more than 10 days). Hearts were then thawed, placed in 2.5% glutaraldehyde for 1 min, and set in 5% agarose. The agarose heart blocks were then sectioned from apex to base in 0.75-mm slices using a Vibratome 1000 plus (Products International Inc., St. Louis, MO). After sectioning, slices were placed overnight in 10% formaldehyde at room temperature before transferring into PBS for 4 h at 4 °C. Sections were then compressed with the spacer plate (0.75 mm) and scanned with Epson scanner. Planimetry was carried out using image analysis software (National Institutes of Health Image version 1.61) and surface area of the whole, and TTC-negative left ventricular myocardium was transformed to volume by multiplication with tissue thickness. Within each heart, after summation of individual slices, TTC-negative infarction volume was expressed as a percentage of left ventricular volume.

RESULTS

Characterization of I/R Porcine Model

The pigs used in this study had similar body weight and heart weight (supplemental Table 1). Pig hearts were subjected to I/R, and tissue was collected 3 (3 I/R) or 15 days (15 I/R) later. The control heart tissue was collected from healthy age-related pigs. The infarct zone was located close to the anterior descending coronary artery, immediately above the apex (Fig. 1*A*). 3 days post-I/R, the infarct area was 525 ± 249 mm^2, which increased to 1069 ± 707 mm^2 by day 15 (Fig. 1*A*, $p < 0.05$). Consistent with this progressive loss of contracting myocardial tissue, there was also a concomitant time-dependent decrease in LV wall thickness as well, significantly reducing from 12.0 ± 1.8 mm in controls to 6.9 ± 2.5 mm in the 15 I/R group (Fig. 1*B*, $p < 0.05$). Samples of surviving myocardium were taken 1 cm away from the infarct zone. Histological analysis of this tissue by staining with hematoxylin and eosin as well as Masson's trichrome verified the absence of fibrosis in all groups (Fig. 1*C*). Samples of this surviving myocardium were taken for proteomic analyses in which protein expression was compared with control samples collected from the same anatomical location in control hearts.

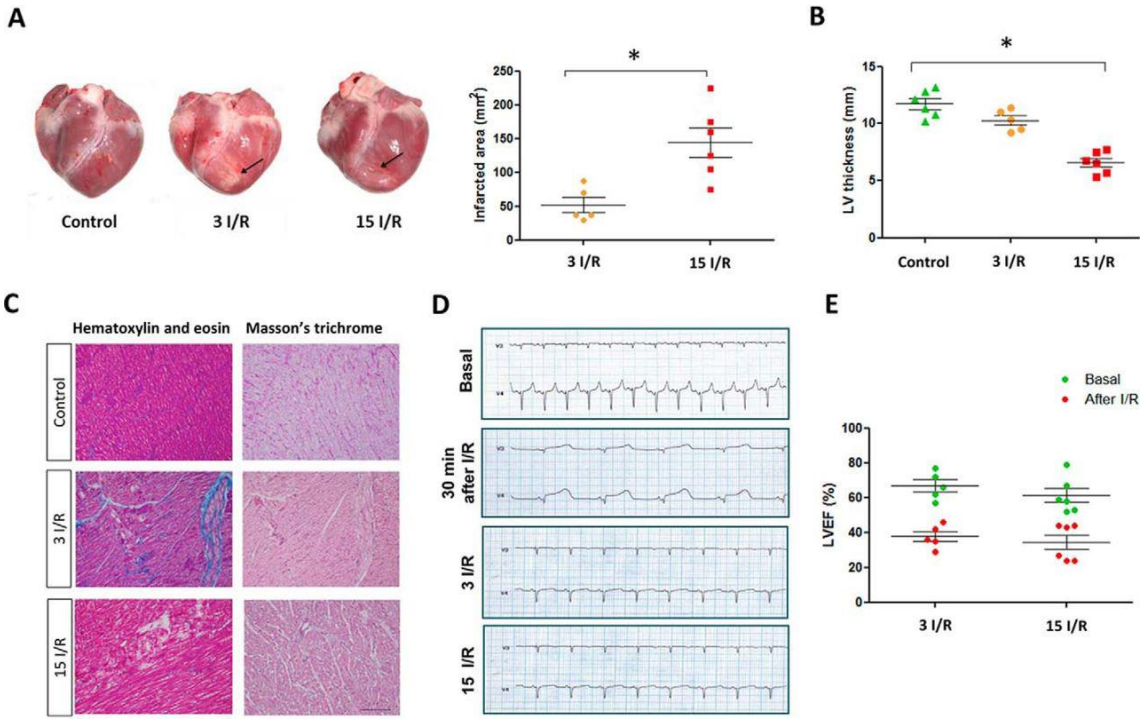

Fig. 1. Characterization of I/R in the porcine model. *A*, representative pig hearts 3 days (3 I/R) and 15 days (15 I/R) after IR injury. *Rows* indicate the infarcted zone. Infarcted area (mm^2) 3 days (3 I/R) and 15 days (15 I/R) after I/R. *B*, left ventricle thickness (in mm). *C*, Masson's trichrome and hematoxylin and eosin staining in control and infarcted hearts. Magnification ×10. *Scale bar*, 200 μm. *D*, representative electrocardiograms before the surgery and 30 min and 3 and 15 days after the IR. The baseline before ischemia shows normal sinus rhythm. Immediately after I/R, an ST elevation in anterior leads V 3–4 was observed. The electrocardiograms 3 and 15 days post-I/R injury indicate a reverse of the ST changes in the anterior and negative T waves in lateral leads. *E*, left ventricular ejection fraction before and 3 and 15 days after I/R. The LVEF was significantly reduced compared against the respective basal levels. * indicates *p* value<0.05.

Electrocardiograms obtained 30 min after I/R showed the typical profile of myocardial injury with ST segment elevation observed in the affected area as monitored by leads V3 and V4. Electrocardiograms showed a loss in electrical conduction in the anterior left ventricle 3 and 15 days after I/R (Fig. 1*D*). At baseline, the LV ejection fraction (LVEF) was above 60% in all animals. However, by 3 or 15 days post-I/R, the LVEF was significantly reduced to 29% ($p < 0.05$) and 27% ($p < 0.001$), respectively (Fig. 1*E*). There was no significant difference in the LVEF between the 3 I/R and 15 I/R group, despite a larger infarct at the latter time point.

Changes in Mitochondrial Protein Expression in Surviving Myocardium Post-I/R

Efficient mitochondrial separation from other cellular compartments was confirmed by Western blot analysis after the stepwise extraction process from heart tissue (supplemental Fig. 1). The proteomic analysis showed the presence of 442 individual mitochondrial proteins, with assignment of each identification being dependent on the minimum of two high confidence peptides being present (supplemental Tables 2 and 3). 85% of the proteins identified had a molecular mass less than 60 kDa, consistent with mitochondrial proteins typically having a lower molecular mass than the cell-wide proteome (18).

Principal component analysis was performed on the proteomics dataset. As expected, the first two principal components responded primarily to differences between the three experimental groups, producing a clear separation between each of them (Fig. 2*A*). However, no differences in the variability of the control and the 15 I/R group were apparent between the first principal component (PC1) and the third principal component (PC3) and the second principal component (PC2) plotted against PC3 (Fig. 2, *B* and *C*). Thus, the variance between groups was largely based on PC1 and PC2, which included 56.08% of the total value (Fig. 2*D*).

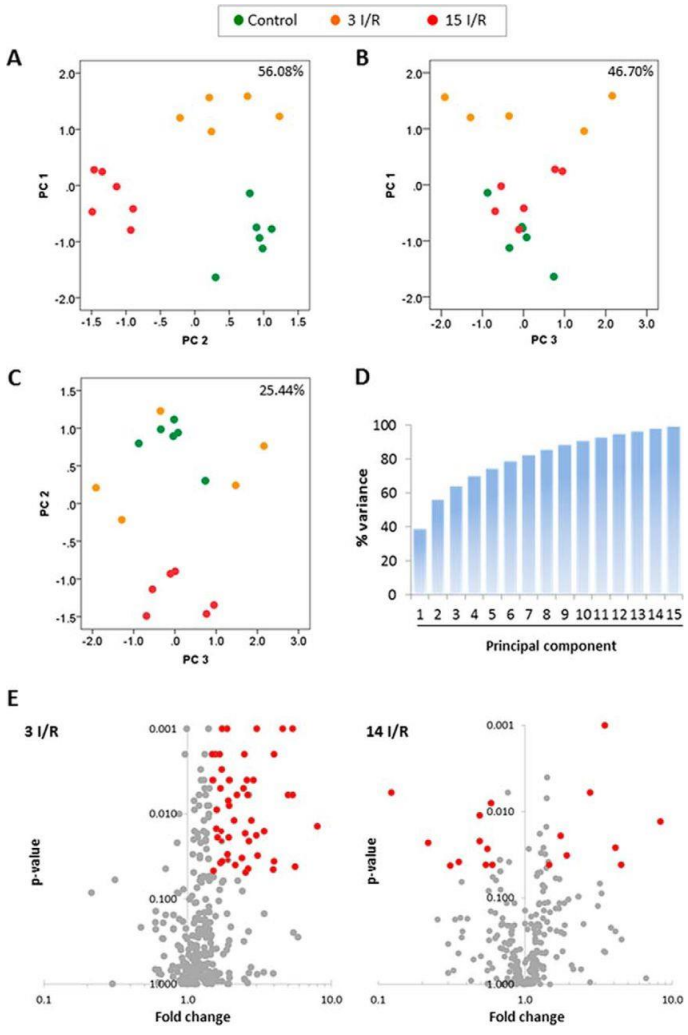

Fig. 2. **Principal component analysis and volcano plots.** The *graphs* represent the percentage of variability explained by the PC1 against PC2 (*A*), the PC1 against PC3 (*B*), and the PC2 against PC3 (*C*). The analysis is based on the differentially expressed proteins identified. Data points represent individual biological replicates (control, $n = 6$; 3 I/R, $n = 5$; 15 I/R, $n = 6$). *D*, cumulative variance graph for all principal components. *E*, volcano plots 3 (3 I/R) and 15 days (15 I/R) after I/R. The normalized peptide counts of each mitochondrial protein in the 3 I/R and 15 I/R groups were compared against controls. Each point represents an individual protein. The significant differences ($p < 0.05$ and fold change ≥ 1.5 or ≤ 0.5) are indicated in *red*.

After the proteomics dataset was normalized by spectral count, 99 proteins were found to be differentially expressed in at least one of the groups (supplemental Table 4). Volcano scatter plots were used to visually highlight the proteins that showed a statistically significant ≥1.5-fold increase or ≥1.5-fold decrease in expression in the 3 I/R or the 15 I/R group relative to the control (Fig. 2*E*).

Expression Changes in Redox Homeostasis and Energy-generating Proteins

The heat map shown in Fig. 3 illustrates that mitochondrial proteins involved in several biological processes showed altered expression 3 or 15 days after I/R. In the 3 I/R group, these included overexpression of proteins responsible for maintaining cellular redox homeostasis (*e.g.* GLRX5 and SOD2), as well as stress adaptation (*e.g.* CH60 and CH10). The 3 I/R group also showed elevated expression of VDAC1 and ADT3, which are involved in the release of pro-apoptotic products from the mitochondria. The most prominent change to the mitochondrial proteome in the surviving myocardium after the I/R intervention was to energy metabolism proteins. For example, the 3 I/R group showed a decrease in proteins that specifically relates to fatty acid catabolism (*e.g.* I3LK72), consistent with the recognized switch away from β-oxidation for energy production in the post-ischemic heart (8). Of particular note was the enhanced expression of BRP44 and BRP44L, which remained significantly elevated in the myocardium 15 days post-I/R. These proteins are subunits of the mitochondrial pyruvate carrier (MPC) responsible for transporting pyruvate, the final product of glycolysis, into the mitochondrial matrix (13, 14).

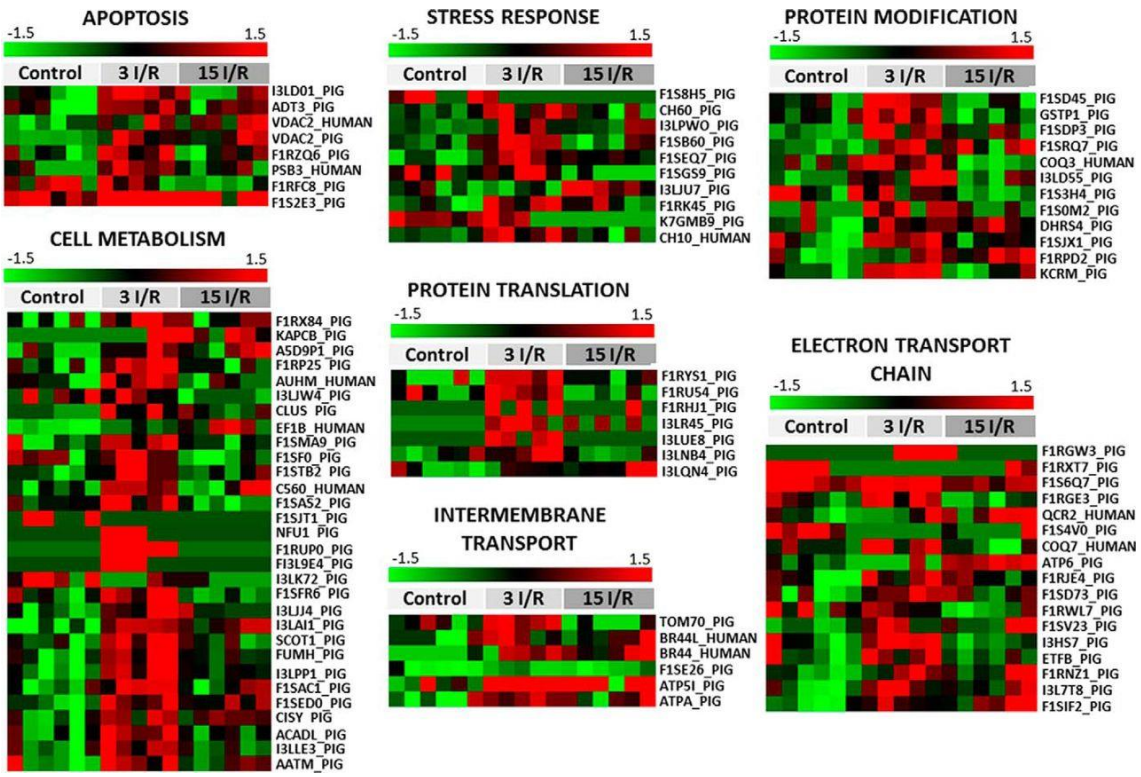

Fig. 3. **Mitochondrial proteins differentially expressed after IR grouped by cellular processes.** *Green-red* heat map values correspond to low-high protein expression levels. The protein normalized value is indicated for each sample. 3 I/R and 15 I/R indicate ischemia/reperfusion with euthanasia after 3 and 15 days, respectively. Fifty seven proteins were differentially expressed 3 days after I/R, 36 of which represented increased expression. However, by 15 days post-I/R, the altered expression observed at 3 days had resolved and normalized back toward the profile of healthy tissue in healthy controls. Thus, 15 days after I/R only, 22 proteins remained differentially expressed, and these included an equal mix of over- or underexpressed proteins. The color track represents the *z*-score for each protein and is scaled from −1.5 (*green*) for down-regulated proteins and 1.5 (*red*) for up-regulated proteins.

These expression changes in MPC, along with the decrease in fatty acid catabolic enzymes mentioned, represent the molecular changes that underlie metabolic shift from fatty acid oxidation to glycolysis after I/R. Parallel to this increase in MPC were increases in several proteins that participate in the Krebs cycle (*e.g.* FUMH, A5D9P1, F1SMA9, C560, I3LPP1, and F1SED0), which are required for the generation of reduced nicotinamide adenine dinucleotide (NADH) and reduced flavin adenine dinucleotide (FADH), which is utilized by the ETC during ATP production. Indeed, ETC proteins (*e.g.* F1RGE3, F1SD73, F1RWL7, and F1SV23) were also elevated 3 days post-infarct. At this time there was also an increase in protein translation machinery (*e.g.* F1RYS1, F1RU54, and I3LR45) and post-translational polypeptide processing enzymes (*e.g.* GSTP1, F1SJX1, and KCRM).

Validation of Proteomic Data

Up-regulation of MPC1 (BRP44L), MPC2 (BRP44), HSP60 (CH60), LONP1, and VDAC1 in three I/R myocardial samples was confirmed by immunoblotting. Although the proteomic analysis of the 15 I/R group had not indicated there was significant differential expression of VDAC1 or BRP44L, quantitative Western immunoblot analysis revealed these proteins were indeed present at elevated levels (Fig. 4*A*). Immunohistochemical analysis also corroborated the increased expression of MPC1 (BRP44L) and MPC2 (BRP44) in the surviving tissue adjacent to the infarct, both at 3 and 15 days post-I/R (Fig. 4*B*). Using real time polymerase chain reaction analysis, we detected an up-regulation of genes that code for MPC1 (BRP44L) and HSP60 in the 3 I/R and 15 I/R groups (Fig. 4*C*).

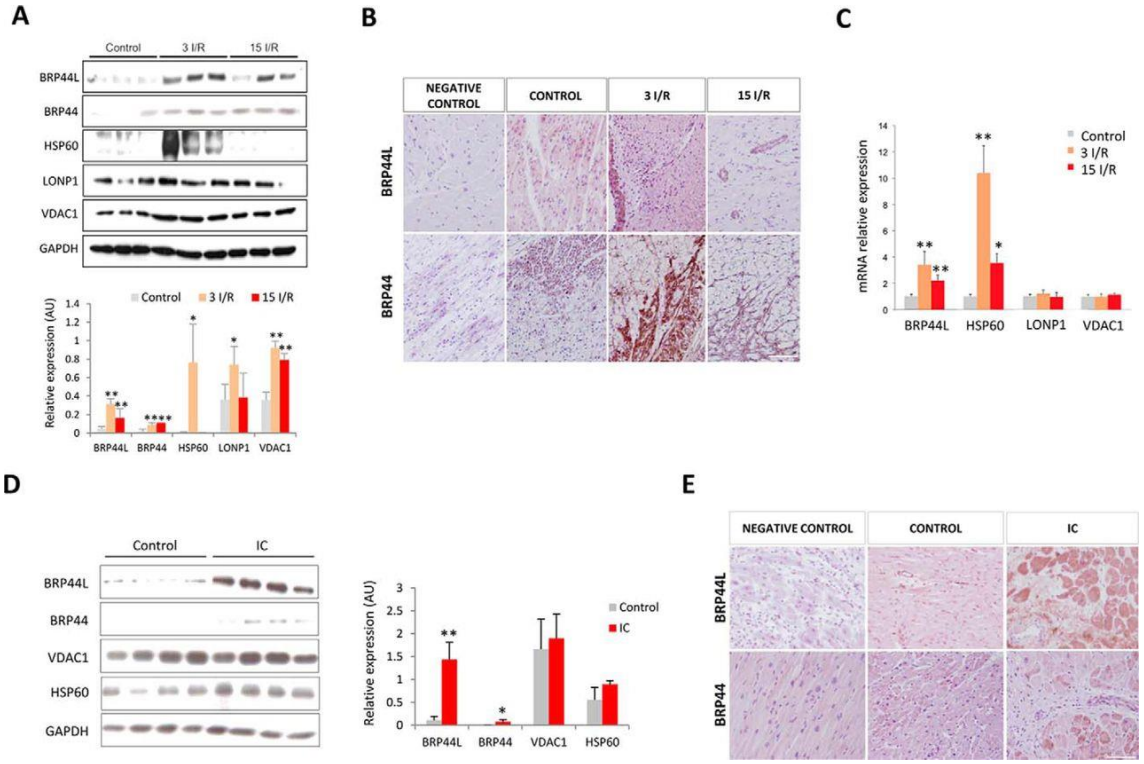

Fig. 4. **Validation of the proteomic data by alternative techniques in the porcine model and in heart tissue from ischemic cardiomyopathy (*IC*) patients.** *A*, Western blot and quantitative densitometry confirming overexpression of BRP44L, BRP44, HSP60, LONP1, and VDAC1 in the border zone from porcine heart samples. The protein normalized value is indicated for each sample. *B*, immunohistochemistry of paraffin-embedded pig heart tissue in the healthy control group, close to the infarcted area, 3 (3 I/R) and 15 days (15 I/R) after I/R. *C*, BRP44L, HSP60, LONP1, and VDAC1 mRNA levels in the same porcine zones. *D*, Western blot analysis and quantitative densitometry of BRP44L, BRP44, VDAC1, and HSP60 expression in heart tissue from healthy donors (*Control*) and patients undergoing cardiac heart transplantation. The normalized protein value is indicated for each sample. *E*, immunohistochemistry of paraffin-embedded healthy and human heart tissue close to the infarcted area. *Scale bar*, 50 μm; * indicates p value <0.05; ** indicates p value <0.001.

MPC1 and MPC2 Are Up-regulated in Patients with Ischemic Heart Failure

Western immunoblot analyses showed MPC1 (BRP44L), MPC2 (BRP44), VDAC1, and HSP60 was also present at elevated levels in cardiac tissue from human patients with ischemic heart failure (Fig. 4*D*). The elevated levels of MPC1 (BRP44L) and MPC2 (BRP44) are in accordance with the similar increases observed in the porcine model. Immunohistochemical analyses further confirmed MPC1 (BRP44L) and MPC2 (BRP44) is present at higher levels in myocardial tissue from the border infarct zone in patients with advanced ischemic heart disease (Fig. 4*E*).

MPC Inhibition Enhanced Infarction Induced by Ischemia and Reperfusion in a Mouse Model

To investigate the impact of mitochondrial pyruvate uptake on myocardial survival following I/R, isolated, perfused mouse hearts were subjected to ischemia and then reperfused in the presence or absence of UK5099, which is an inhibitor of the MPC. This pharmacological inhibition of uptake significantly increased infarct size (Fig. 5*A*) and also worsened recovery of ventricular function. The left ventricular pressure was lower (Fig. 5*B*), and the left ventricular end diastolic pressure was higher in the hearts treated with UK5099 (Fig. 5*C*). In contrast, UK5099 did not have any adverse effects on aerobically perfused hearts, although it did elevate cytosolic pyruvate and lactate, consistent with inhibition of MPC-dependent mitochondrial uptake of pyruvate (supplemental Fig. 2). Coronary flow was similar in both groups (Fig. 5*D*).

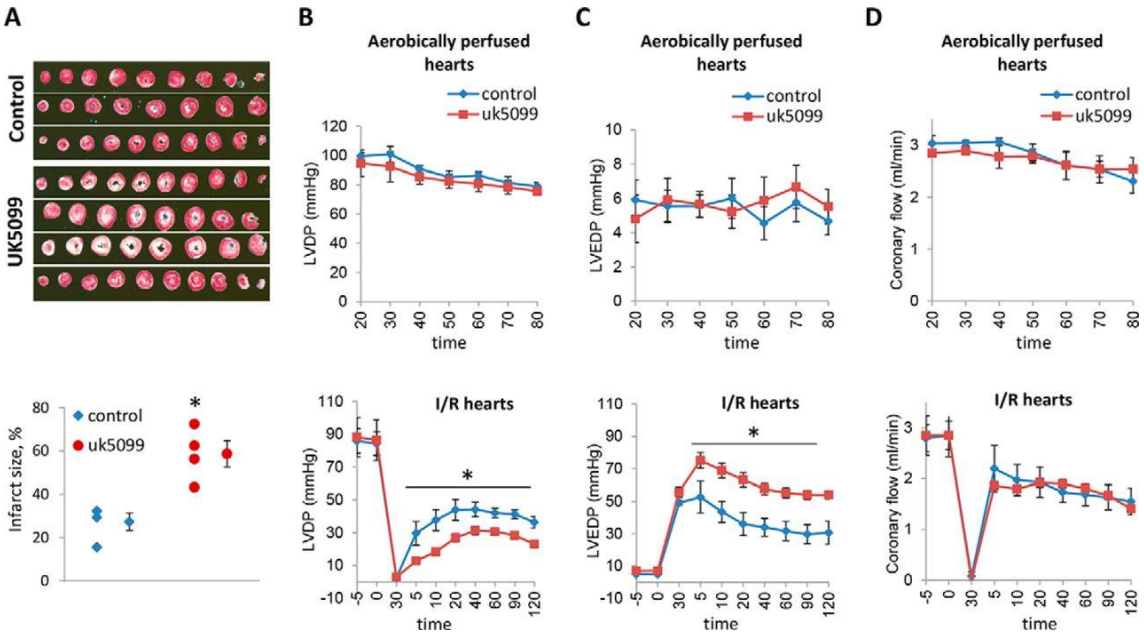

Fig. 5. **Mitochondrial pyruvate carriers inhibition increases the infarct size after I/R in a mouse model.** Langendorff-perfused mouse hearts were subjected to aerobic perfusion with modified Krebs solution in order to examine the toxicity of the mitochondrial pyruvate carrier inhibitor UK5099 (50 μm). The mouse hearts were subjected to 30 min of no-flow global ischemia followed by 120 min of reperfusion. Modified Krebs solution (*Control*) or Krebs solution with UK5099 (50 μm) was perfused for 120 min after ischemia. *A*, representative photographs of 2,3,5-triphenyltetrazolium chloride-stained mouse heart sections obtained after the I/R protocol and *graph* showing infarct size expressed as percentage of total ischemic area in each group. Cardiac function is presented as *B*. Left ventricular developed pressure (*LVDP*, mm Hg) (*B*) and left ventricular end diastolic pressure (*LVEDP*, mm Hg) (*C*) are shown. *D*, coronary flow (ml/min). Values are means ± S.E.; control group, $n = 3$. UK5099 group $n = 4$. * indicates p value <0.05.

DISCUSSION

Mitochondrial function and energetics are important determinants of myocardial viability after I/R that can lead to infarction and progress to heart failure. Most proteomic studies assessing mitochondrial changes in the setting of I/R, either acutely or as heart failure ensues, have used rodent models (19). Here we utilized a large animal, a porcine model that may be more relevant to the pathogenesis of human heart disease. We specifically focused on changes to the mitochondria that occur in tissue in a precisely anatomically defined location proximal to the site of infarction but had survived and was viable as confirmed by histological analysis. Past studies have primarily described mitochondrial proteome changes using less precisely defined tissues in which there is likely heterogeneity in cell viability (20, 21). We were specifically interested in tissue that remained viable despite having been at risk of necrosis, because changes to the mitochondrial proteome may have impacted survival. By identifying such adaptive changes that protect the heart, this may provide important insight to target proteins that new therapeutic interventions could be aimed at to limit necrosis and the transition to failure following I/R.

We defined the basal mitochondrial proteome of healthy hearts not subjected to I/R, and we determined how this was altered in the surviving myocardium 3 or 15 days after the infarct-inducing protocol. There were substantive and dynamic changes in protein expression in the heart tissue that survived. For example, within the two post-I/R groups together, 99 mitochondrial proteins showed altered expression relative to control. The most prominent changes were observed 3 days after I/R, with the expression profile having markedly resolved back toward basal by day 15. The changes 3 days after I/R were dominated by proteins that become overexpressed compared with those changing to have reduced expression.

VDAC1 and ATD3, proteins that can induce mitochondrial permeability to promote cell death by apoptosis (22, 23), showed enhanced expression on day 3 after I/R. Histological analysis had confirmed that the tissue samples were healthy; thus, despite the elevated expression of these proteins, apoptosis was absent. Indeed, this tissue was also characterized by overexpression of protective heat shock proteins such as HSP60, CH10, and F1SB60 (SOD2). These proteins are increased during I/R (24, 25) and can limit injury by preventing protein aggregation or ensuring correct assembly of newly synthesized proteins. HSP60 is particularly notable because it maintains mitochondrial integrity and capacity for ATP generation after I/R (26). Moreover, HSP60 overexpression has been shown to be protective against apoptotic and necrotic cell death (24). The stress protein LONP, which is responsible for degradation of oxidized dysfunctional proteins (27), was also present at higher levels. This may be due to a need to clear damaged proteins during the acute phase of injury at day 3, which is likely to have passed by day 15 when LONP levels returned to basal.

Three days after I/R, another set of proteins showing marked overexpression were members of the ETC family (F1RGE3, F1SD73, F1RWL7, and F1SV23). This reflects an increased energy demand, required to compensate for the increased contractile work load this viable tissue is under due to proximity to the infarct that can no longer contribute to cardiac output. Enhanced energy production may also be needed for repair and stress-adaptive responses to maintain viability. Consistent with enhanced expression of ETC proteins, there were parallel increases in Krebs cycle proteins (FUMH, A5D9P1, F1SMA9, C560, I3LPP1, and F1SED0). This will potentiate generation of NADH, which is consumed by the ETC during ATP production.

The healthy heart uses β-oxidation of fatty acids as it predominant mechanism of energy production (28, 29). However, when oxygen and blood flow are interrupted during ischemia, there is a shift to glycolysis, a more efficient energy-yielding pathway in terms of oxygen utilization (5, 6). Consistent with the established switch from β-oxidation of fatty acids to glycolytic substrates BRP44 and BRP44L, expression was elevated at both 3 and 15 days after I/R in the surviving tissue in the post-ischemic heart. These proteins were recently renamed as MPC1 and MPC2 (13, 14), reflecting their identification as subunits of the MPC, which is responsible for transporting pyruvate, the final product of glycolysis, into the mitochondrial matrix. Conversely, ischemia induced the overexpression of AATM or ACADL, which are involved in fatty acids metabolism. It has been shown that fatty acid accumulation can up-regulate specific genes involved in fatty acid transport *in vivo*. For example, the gene that encodes ACADL was up-regulated in the heart in response to a high fat diet (31), suggesting that despite the metabolic shift to glycolysis after ischemia, the accumulation of fatty acids inside the cell could up-regulate the transcription of genes involved in β-oxidation.

Overall, the molecular expression changes that we have unveiled using an unbiased proteomic screen provide a molecular rationalization of the well documented switch of the post-ischemic heart from β-oxidation to glycolysis. The metabolic shift to glycolytically derived ATP production increases the concentration of pyruvate in the cytoplasm. If this cytosolic pyruvate is not subsequently oxidized, there is a net production of protons that contributes to ischemia-induced acidosis (32). This intracellular acidosis may contribute to several potentially adverse events, including intracellular Na^+ and Ca^{2+} overload, decreased responsiveness of contractile proteins to Ca^{2+} that depresses cardiac output and initiation of arrhythmias (33). Therefore, the elevation in MPC1 and MPC2 may limit tissue injury by enhancing uptake of pyruvate to limit intracellular acidosis. Indeed, when glycolytically derived pyruvate is incorporated into mitochondria and metabolized by pyruvate dehydrogenase or pyruvate carboxylase, the net production of protons from glucose metabolism is zero as those produced by glycolysis are consumed in the Krebs cycle (34). Furthermore, this metabolic switch to glycolysis is more efficient than fatty acid oxidation in terms of oxygen consumption (7). This may be important as systemic oxygen delivery is sub-optimal as a result of the depressed cardiac output post-I/R.

The increased expression of MPC1 and MPC2 in the post-ischemic heart may represent an endogenous mechanism that enhances mitochondrial pyruvic acid uptake to enhance tissue viability. To test the importance of mitochondrial pyruvate uptake for tissue survival and maintenance of cardiac function during I/R, we used an isolated perfused mouse heart model. Mouse hearts were subjected to ischemia and reperfused with or without the MPC inhibitor UK5099. This pharmacological inhibition of pyruvate uptake by MPC during post-ischemic reperfusion exacerbated infarction and worsened recovery of ventricular contractile function, consistent with mitochondrial pyruvate uptake being an important determinant of myocardial tissue survival post-infarct. This is consistent with a wealth of studies that have shown that providing pyruvate at reperfusion is protective (30).

It is intriguing that we also witnessed enhanced expression of MPC1 and MPC2 in the myocardium of human subjects with ischemic heart disease, which presumably may represent an endogenous mechanism to recruit the cardioprotective benefits of enhancing mitochondrial pyruvate uptake described here. At the outset of this study, we hoped to identify changes to the mitochondrial proteome in tissue at risk of necrosis during I/R but survived, as this may provide insight to endogenous mechanisms of protection. Indeed, consistent with this rationale, our observations suggest that interventions that enhance the levels of MPC protein or stimulate its pyruvate transport activity would be of therapeutic value.

Acknowledgments
We thank “Biobanco A Coruña” (INIBIC-CHUAC, Spain) for providing healthy heart tissue samples. We are grateful to Maria Fraga for technical assistance. We appreciate Abel Martin Garrido and Olujimi Oviosu for help with editing the manuscript.

Footnotes
Author contributions: M.F., J.B., and N.D. designed research; M.F., O.P., J.B., R.C., and G.A. performed research; M.G.C., P.E., and N.D. contributed new reagents or analytic tools; M.F., O.P., and J.B. analyzed the data; and M.F., P.E., and N.D. wrote the paper.

REFERENCES

1.↵Marchant, D. J., Boyd, J. H., Lin, D. C., Granville, D. J., Garmaroudi, F. S., and McManus, B. M. (2012) Inflammation in myocardial diseases. Circ. Res. 110, 126–144
2.↵Walters, A. M., Porter, G. A., Jr.., and Brookes, P. S. (2012) Mitochondria as a drug target in ischemic heart disease and cardiomyopathy. Circ. Res. 111, 1222–1236
3.↵Wisneski, J. A., Gertz, E. W., Neese, R. A., Gruenke, L. D., and Craig, J. C. (1985) Dual carbon-labeled isotope experiments using d-[6-14C]glucose and l-[1,2,3-13C3]lactate: a new approach for investigating human myocardial metabolism during ischemia. J. Am. Coll. Cardiol. 5, 1138–1146
4.↵Gertz, E. W., Wisneski, J. A., Stanley, W. C., and Neese, R. A. (1988) Myocardial substrate utilization during exercise in humans: dual carbon-labeled carbohydrate isotope experiments. J. Clin. Invest. 82, 2017–2025
5.↵Wambolt, R. B., Henning, S. L., English, D. R., Dyachkova, Y., Lopaschuk, G. D., and Allard, M. F. (1999) Glucose utilization and glycogen turnover are accelerated in hypertrophied rat hearts during severe low-flow ischemia. J. Mol. Cell. Cardiol. 31, 493–502

6. Renstrom, B., Liedtke, A. J., and Nellis, S. H. (1990) Mechanisms of substrate preference for oxidative metabolism during early myocardial reperfusion. Am. J. Physiol. 259, H317–H323
7. Tuunanen, H., and Knuuti, J. (2011) Metabolic remodelling in human heart failure. Cardiovasc. Res. 90, 251–257
8. Buerke, M., Schwertz, H., Längin, T., Buerke, U., Prondzinsky, R., Platsch, H., Richert, J., Bomm, S., Schmidt, M., Hillen, H., Lindemann, S., Blaschke, G., Müller-Werdan, U., and Werdan, K. (2006) Proteome analysis of myocardial tissue following ischemia and reperfusion-effects of complement inhibition. Biochim. Biophys. Acta 1764, 1536–1545
9. Urbonavicius, S., Wiggers, H., Bøtker, H. E., Nielsen, T. T., Kimose, H. H., Østergaard, M., Lindholt, J. S., Vorum, H., and Honoré, B. (2009) Proteomic analysis identifies mitochondrial metabolic enzymes as major discriminators between different stages of the failing human myocardium. Acta Cardiol. 64, 511–522
10. Heinke, M. Y., Wheeler, C. H., Chang, D., Einstein, R., Drake-Holland, A., Dunn, M. J., and dos Remedios, C. G. (1998) Protein changes observed in pacing-induced heart failure using two-dimensional electrophoresis. Electrophoresis 19, 2021–2030
11. White, M. Y., Cordwell, S. J., McCarron, H. C., Prasan, A. M., Craft, G., Hambly, B. D., and Jeremy, R. W. (2005) Proteomics of ischemia/reperfusion injury in rabbit myocardium reveals alterations to proteins of essential functional systems. Proteomics 5, 1395–1410
12. Barallobre-Barreiro, J., Didangelos, A., Schoendube, F. A., Drozdov, I., Yin, X., Fernández-Caggiano, M., Willeit, P., Puntmann, V. O., Aldama-López, G., Shah, A. M., Doménech, N., and Mayr, M. (2012) Proteomics analysis of cardiac extracellular matrix remodeling in a porcine model of ischemia/reperfusion injury. Circulation 125, 789–802
13. Bricker, D. K., Taylor, E. B., Schell, J. C., Orsak, T., Boutron, A., Chen, Y. C., Cox, J. E., Cardon, C. M., Van Vranken, J. G., Dephoure, N., Redin, C., Boudina, S., Gygi, S. P., Brivet, M., Thummel, C. S., and Rutter, J. (2012) A mitochondrial pyruvate carrier required for pyruvate uptake in yeast, Drosophila, and humans. Science 337, 96–100
14. Herzig, S., Raemy, E., Montessuit, S., Veuthey, J. L., Zamboni, N., Westermann, B., Kunji, E. R., and Martinou, J. C. (2012) Identification and functional expression of the mitochondrial pyruvate carrier. Science 337, 93–96
15. Ryou, M. G., Liu, R., Ren, M., Sun, J., Mallet, R. T., and Yang, S. H. (2012) Pyruvate protects the brain against ischemia-reperfusion injury by activating the erythropoietin signaling pathway. Stroke 43, 1101–1107
16. Mallet, R. T., and Sun, J. (1999) Mitochondrial metabolism of pyruvate is required for its enhancement of cardiac function and energetics. Cardiovasc. Res. 42, 149–161
17. Shevchenko, A., Tomas, H., Havlis, J., Olsen, J. V., and Mann, M. (2006) In-gel digestion for mass spectrometric characterization of proteins and proteomes. Nat. Protoc. 1, 2856–2860
18. Taylor, S. W., Fahy, E., Zhang, B., Glenn, G. M., Warnock, D. E., Wiley, S., Murphy, A. N., Gaucher, S. P., Capaldi, R. A., Gibson, B. W., and Ghosh, S. S. (2003) Characterization of the human heart mitochondrial proteome. Nat. Biotechnol. 21, 281–286
19. Cosme, J., Emili, A., and Gramolini, A. O. (2013) Large-scale characterization of the murine cardiac proteome. Methods Mol. Biol. 1005, 1–10
20. Lagranha, C. J., Deschamps, A., Aponte, A., Steenbergen, C., and Murphy, E. (2010) Sex differences in the phosphorylation of mitochondrial proteins result in reduced production of reactive oxygen species and cardioprotection in females. Circ. Res. 106, 1681–1691
21. Shinmura, K., Tamaki, K., Sano, M., Nakashima-Kamimura, N., Wolf, A. M., Amo, T., Ohta, S., Katsumata, Y., Fukuda, K., Ishiwata, K., Suematsu, M., and Adachi, T. (2011) Caloric restriction primes mitochondria for ischemic stress by deacetylating specific mitochondrial proteins of the electron transport chain. Circ. Res. 109, 396–406
22. Zamzami, N., and Kroemer, G. (2001) The mitochondrion in apoptosis, how Pandora's box opens. Nat. Rev. Mol. Cell Biol. 2, 67–71
23. Crompton, M., Barksby, E., Johnson, N., and Capano, M. (2002) Mitochondrial intermembrane junctional complexes and their involvement in cell death. Biochimie 84, 143–152
24. Lau, S., Patnaik, N., Sayen, M. R., and Mestril, R. (1997) Simultaneous overexpression of two stress proteins in rat cardiomyocytes and myogenic cells confers protection against ischemia-induced injury. Circulation 96, 2287–2294
25. Martin, J. L., Mestril, R., Hilal-Dandan, R., Brunton, L. L., and Dillmann, W. H. (1997) Small heat shock proteins and protection against ischemic injury in cardiac myocytes. Circulation 96, 4343–4348
26. Welch, W. J., Kang, H. S., Beckmann, R. P., and Mizzen, L. A. (1991) Response of mammalian cells to metabolic stress; changes in cell physiology and structure/function of stress proteins. Curr. Top. Microbiol. Immunol. 167, 31–55
27. Bulteau, A. L., Lundberg, K. C., Ikeda-Saito, M., Isaya G., and Szweda, L. I. (2005) Reversible redox-dependent modulation of mitochondrial aconitase and proteolytic activity during in vivo cardiac ischemia/reperfusion. Proc. Natl. Acad. Sci. U.S.A. 102, 5987–5991
28. Neely, J. R., and Morgan, H. E. (1974) Relationship between carbohydrate and lipid metabolism and the energy balance of heart muscle. Annu. Rev. Physiol. 36, 413–459
29. Zhang, L., Keung, W., Samokhvalov, V., Wang, W., and Lopaschuk, G. D. (2010) Role of fatty acid uptake and fatty acid beta-oxidation in mediating insulin resistance in heart and skeletal muscle. Biochim. Biophys. Acta 1801, 1–22
30. Hasenfuss, G., Maier, L. S., Hermann, H. P., Lüers, C., Hünlich, M., Zeitz, O., Janssen, P. M., and Pieske, B. (2002) Influence of pyruvate on contractile performance and Ca2+ cycling in isolated failing human myocardium. Circulation 105, 194–199

31. Ouali, F., Djouadi, F., Merlet-Bénichou, C., Riveau, B., and Bastin, J. (2000) Regulation of fatty acid transport protein and mitochondrial and peroxisomal β-oxidation gene expression by fatty acids in developing rats. Pediatr. Res. 48, 691–696
32. Liu, Q., Docherty, J. C., Rendell, J. C., Clanachan, A. S., and Lopaschuk, G. D. (2002) High levels of fatty acids delay the recovery of intracellular pH and cardiac efficiency in post-ischemic hearts by inhibiting glucose oxidation. J. Am. Coll. Cardiol. 39, 718–725
33. Carmeliet, E. (1999) Cardiac ionic currents and acute ischemia: from channels to arrhythmias. Physiol. Rev. 79, 917–1017
34. Dennis, S. C., Gevers, W., and Opie, L. H. (1991) Protons in ischemia: where do they come from; where do they go to? J. Mol. Cell. Cardiol. 23, 1077–1086